

INFLUENCE OF ASPECT RATIO OF TEMPO-OXIDIZED CELLULOSE NANOFIBERS (TOCNs) FROM WOOD PULP ON POLYMERIC MEMBRANE PROPERTIES

NOVITRI HASTUTI,^{***} DIAN ANGGRAINI INDRAWAN,^{*}
KYOHEI KANOMATA^{***} and TAKUYA KITAOKA^{****}

^{*}Research Center for Biomass and Bioproducts, National Research and Innovation Agency (BRIN),
Soekarno Science Center Cibinong, Jalan Raya Jakarta – Bogor KM 46,
Cibinong, Bogor, Jawa Barat, 16911, Indonesia

^{**}Research Collaboration Center for Nanocellulose BRIN-Universitas Andalas,
Padang, 25163, Indonesia

^{***}Graduate School of Pharmaceutical Sciences, Osaka University, 1-6 Yamadaoka,
Suita-shi, Osaka, 565-0871, Japan

^{****}Department of Agro-Environmental Sciences, Faculty of Agriculture, Kyushu University,
Motoooka 744 Nishi-ku, 8190395, Fukuoka, Japan

✉ Corresponding author: N. Hastuti, novi043@brin.go.id

Received April 20, 2023

The incorporation of TEMPO-oxidized cellulose nanofibers (TOCNs) derived from wood pulp resulted in an improvement in the characteristics of polymeric membranes made up of poly (methyl vinyl ether maleic acid)/PMVEMA and poly (ethylene glycol)/PEG. The membranes were constructed, and TOCNs were included in the formulation at a rate of 5 wt%. TOCNs were categorized as either short or long, depending on the aspect ratio measurement. According to the findings of the research, the various lengths of TOCNs resulted in variances in the optical transmittance properties, contact angles, and whiteness level of the membranes, in addition to a little variation in the tensile and thermal properties of the material. When compared to short TOCNs, long TOCNs offer somewhat improved performance in terms of optical transmittance, whiteness level, tensile characteristics, and thermal stability. The results of this study reveal the significance of the morphology of nanocellulose in determining the properties of the composite that includes it. Thus, the characteristics of the target membrane were greatly influenced by nanocellulose morphology.

Keywords: cellulose, fibres, membrane, nanocellulose, wood pulp

INTRODUCTION

Nanocelluloses (NC) are frequently added to polymeric systems to improve their mechanical, rheological, and barrier properties.¹ The use of NC in polymer matrices improves not only mechanical qualities, but also anti-biofouling, thermal, and gas barrier properties.²⁻⁵ Several NC parameters, including structural morphology, crystallinity, aspect ratio, and surface chemistry, influenced NC performance in polymer matrices.⁶⁻⁹

In addition, the qualities of natural fibers rely on their source and the conditions of their extraction.^{10,11} Chen and co-authors¹² have also described the use of NC as a reinforcing agent

from various non-wood fibers. The investigation found that bamboo nanofibers had the greatest reinforcing impact on the starch film, because they had the highest aspect ratio, although having less crystallinity than cotton linter and sisal.¹²

It was also found that the various types of NC applied to the polymer matrix exhibited distinct performances. Cellulose nanocrystals (CNCs) and cellulose nanofibrils (CNFs) added as reinforcing agents into a poly (hydroxybutyrate-co-hydroxy valerate)/PHBV matrix revealed that both boosted the tensile characteristics of the PHBV composite, with CNCs exhibiting a more pronounced reinforcing effect than CNFs.¹³ TEMPO-oxidized

cellulose nanofibrils (TOCNs) exhibited a high tensile modulus and thermal stability in poly (vinyl alcohol) and polyvinyl fluoride (PVDF) matrices.^{2,14} In previous studies, the use of NC as reinforcing filler in a PMVEMA-PEG matrix was developed in concentrations of 25-75%.^{15,16} In addition, Goetz *et al.* reported the fabrication of films composed of cross-linked PMVEMA/PEG/CNCs. The films exhibited notable water absorption properties, suggesting that the cross-linking of nanocellulosics with a water-soluble biopolymer matrix, specifically PMVEMA/PEG, led to the formation of a uniformly dispersed nano-composite that demonstrated stability in an environment containing water.¹⁵ The matrix and cellulose nanowhiskers are intended to form cross-linked networks that inhibit aggregation and create unique mechanical properties in the nanocomposites. The results reveal that *in situ* cross-linking of cellulose nanowhiskers with a matrix polymer yields nanocomposites with well-dispersed nanowhiskers, customized nanostructure, and mechanical performance.¹⁷ Nevertheless, this investigation solely examined the impact of nanocellulose concentration, without considering variations in the morphology of the nanocellulose employed.

This work seeks to discover if changes in the morphology of nanocellulose, namely length, influence the characteristics of the membrane incorporating TEMPO-oxidized cellulose nanofibers (TOCNs). Furthermore, TEMPO oxidation is a well-known method for producing nanocellulose, which yields cellulose nanofibers that are highly individualized. These nanofibers have a width of approximately 3-4 nm and a length of at least a few microns.¹⁸ In addition, native celluloses like bleached wood pulp and cotton undergo surface oxidation, which preserves the fibrous structure of the pulp.¹⁹ The oxidation process resulted in the selective conversion of nearly all primary hydroxyl groups of cellulose to carboxyl groups, yielding a highly pure form of β -1,4-linked polyglucuronic acid sodium salt, also known as cellouronic acid Na salt.^{20,21} Carboxyl groups on microfibril surfaces have negative charges in water, leading to repulsion between microfibrils. As a result, oxidized pulp can be completely broken down into individual microfibrils through gentle mechanical treatment in water.^{19,22} An increase in carboxyl content in oxidized pulps is expected to affect the physical properties of the handsheets.²¹

Previous research has demonstrated the potential of PMVEMA/PEG films for use in bio-adhesive patch-based systems incorporating aminolevulinic acid for photodynamic therapy.²³ In addition, a study demonstrated that the PMVEMA/PEG hydrogel has potential for cell culture. It exhibited improved cytocompatibility and effectively supported the growth of HO8910 ovarian cancer cells and the formation of multicellular spheroids in a 3D model.²⁴

Hence, investigating the variations in TOCN morphology on PMVEMA/PEG membranes is anticipated to offer insights into the characteristics of the resulting hydrogels and their potential applications. Thus, the utilization of TOCNs as a filler or membrane framework can be approximated based on the desired membrane properties of PMVEMA/PEG.

EXPERIMENTAL

Materials

TEMPO-oxidized cellulose nanofibers (TOCNs) from Nippon Paper Company, Japan, were denoted as TCS and TCL for short TOCNs and long TOCNs, respectively. The carboxylate contents and aspect ratio were as follows: 1.61 mmol/g and 24 \pm 7 for TCS; and 1.43 mmol/g and 44 \pm 16 for TCL, respectively. The TOCNs were derived from softwood pulp.

This study made use of poly methyl vinyl ether maleic acid/PMVEMA (Mw 1.980.000, Sigma Aldrich, USA), and poly ethylene glycol/PEG, (Mw 20.000, Wako Pure Chemical Industries, Osaka, Japan). To achieve a pH of 2, 0.1 M of hydrochloric acid was utilized in the production of the solution. An Arium Ultrapure Water System was utilized to achieve water purity prior to its use in this investigation (Sartorius Co., Ltd., Tokyo, Japan).

Methods

TEMPO-oxidized cellulose nanofibers (TOCNs) were synthesized from wood pulp according to the method reported earlier.²⁵ Short and long TOCNs were denoted as TCS and TCL, respectively. The carboxylate content was determined using the electric conductivity titration method, as described previously,²⁵ in which a dried sample weighing 0.3 g was combined with 55 mL of water and 5 mL of a 0.01 M NaCl solution. The resulting combination was thoroughly agitated to achieve a well-dispersed slurry. Subsequently, a solution of hydrochloric acid (HCl) with a concentration of 0.1 M was introduced into the combination in order to establish a pH level within the desired range of 2.5-3.0. A solution of sodium hydroxide (NaOH) with a concentration of 0.04 M was gradually introduced at a rate of 0.1 mL per minute until a pH of 11 was reached. This process was facilitated by employing a pH stat. The determination

of the carboxylate content of the sample was conducted based on the analysis of the conductivity and pH curves.

The aspect ratios for TCS and TCL were computed using Image J based on the microscopic pictures obtained by a Transmission Electron Microscope (TEM). The process of membrane production outlined in our earlier paper,²⁶ which refers to the method of L. Goetz *et al.*,¹⁵ consists in a technique involving a decrease in the concentration of nanocellulose employed, specifically to a level of 5 wt%. The total amount of PMVEMA and PEG utilized was 1.5 g, with a ratio of 6.7:1 between PMVEMA and PEG. The PMVEMA polymer was first dissolved in 68 °C, HCl-acidified, distilled water, with a pH of 2, to produce a solution. Following the complete dissolution of PMVEMA, PEG polymer and 5 wt% TOCN suspensions were added (TCS and TCL, respectively). The PMVEMA, PEG, and TOCN polymer mixture solution was mixed continuously for approximately 30 minutes before being put into a Teflon Petri dish and dried at 40 °C for 3–4 days.

TOCNs were subsequently characterized by measuring their length and width using TEM (JEM 2100-HC, JEOL Ltd., Tokyo, Japan), with an acceleration voltage of 120 kV at the Ultramicroscopy Research Centre, Kyushu University. The membrane morphology was observed using Atomic Force Microscopy (AFM) in the scanning probe mode (Dimension Icon with Scan Asyst function); the results were analyzed by NanoScope Analysis Version 1.80. Transmittance properties of the obtained membranes were observed using UV-Vis Spectroscopy (UH5300 Hitachi, Tokyo, Japan) at 250–800 nm wavelength, and contact angles were measured using Drop Master 300 K (Kyowa Interface Science Co, Ltd., Saitama, Japan) by dropping a 1 μ L water droplet in four different spots on the film surface. Thermal properties were observed using thermogravimetric analysis/TGA (TG/DTA 7300, Hitachi, Tokyo, Japan) and mechanical properties were examined using Material Testing Instruments (STA-1225, Orientec Co., Ltd., Tokyo, Japan), equipped with a 100 N load cell, as described in our previous study.²⁶ The whiteness level of the membrane was measured

using a portable colorimeter (NR-3000) (Nippon Denshoku Industries Co., Ltd., Tokyo, Japan). A white standard color plate ($L = 97.75$, $a = -0.49$ and $b = 1.96$) was used as a background for color measurements. Hunter color (L , a , and b) values were averaged from three readings from each sample. Color values were expressed as L^* (whiteness or brightness/darkness), a^* (redness/greenness), and b^* (yellowness/blueness).²⁷ The total color difference (ΔE) was calculated as follows:

$$\Delta E = \sqrt{(\Delta L)^2 + (\Delta a)^2 + (\Delta b)^2} \quad (1)$$

RESULTS AND DISCUSSION

TOCNs morphology

Transmission electron microscopy (TEM) pictures of TEMPO-oxidized cellulose nanofibers (TOCNs) were observed. TEM pictures of the short (TCS) and long (TCL) morphology of TEMPO oxidized cellulose nanofibers (TOCNs) are shown in Figure 1. The photos depict individual nanofibers after oxidation mediated by TEMPO. It is known that these individual nanofibers have a high aspect ratio and are well diffused in water.^{2,28} However, the aspect ratio of the TOCN will be diminished with the application of intensive and more difficult mechanical disintegration.² The carboxylate content and aspect ratio were 1.61 mmol/g and 24 ± 7 , and 1.43 mmol/g and 44 ± 16 , for TCS and TCL, respectively.

Membrane morphology

The morphology of the membranes was examined using atomic force microscopy (AFM) (Fig. 2). AFM microscopy pictures demonstrated that the TOCNs were evenly distributed throughout the membrane matrix. Brighter markings indicate the membrane's highest point or nodule, while darker hues show membrane valleys or pores.²⁹

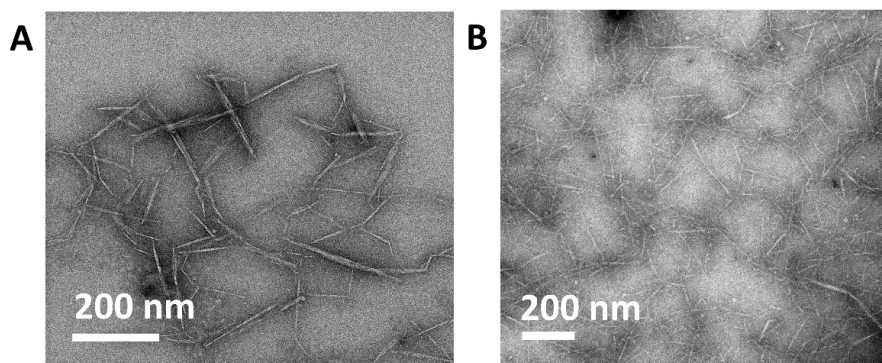


Figure 1: TEM images of (A) TCS and (B) TCL

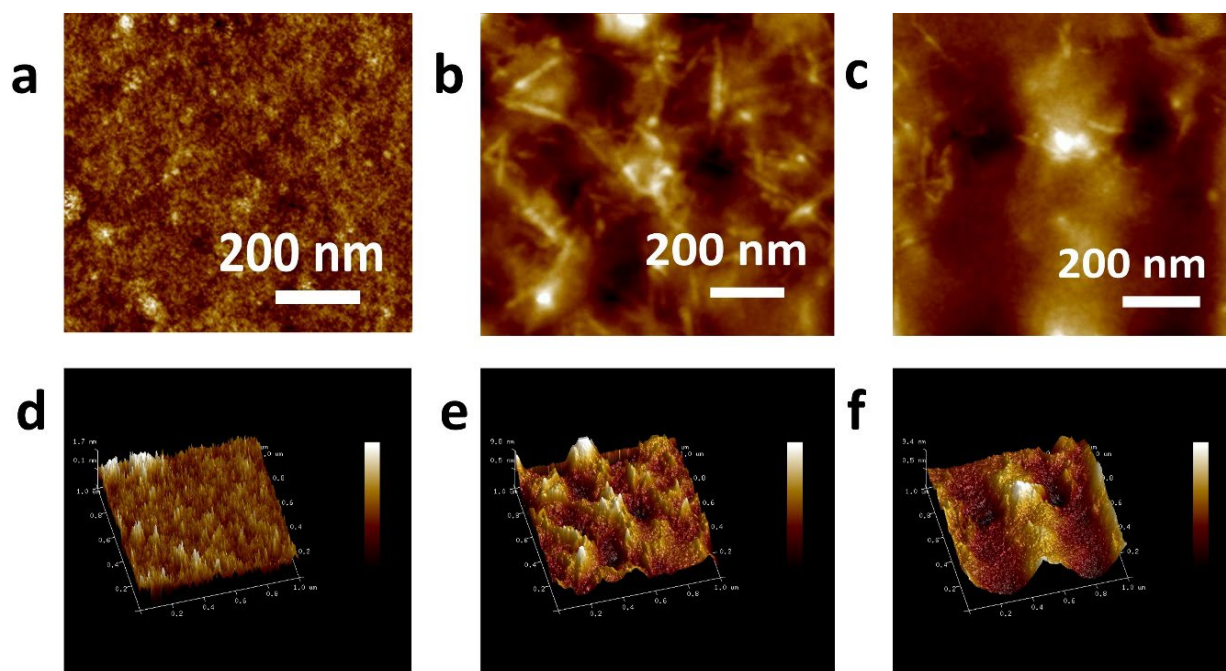


Figure 2: Membrane morphology (upper) and surface roughness of the membranes (bottom) composed of: (a, d) PMVEMA-PEG-only; (b, e) 5 wt% TCL and (c, f) 5 wt% TCS

The average surface roughness (R_a , the mean value of the surface relative to the center plane) of the membranes incorporating short TOCNs and long TOCNs was close to 2. The addition of less than 1.5 wt% TOCNs to cellulose triacetate membranes considerably increased the surface roughness of the membrane.³⁰ The mean roughness (R_a) of the membranes with short TOCNs was not significantly different from that of the membranes with long TOCNs.

Optical transmittance

The light transmittance of TCS and TCL at 550 nm was 73% and 81%, respectively (Fig. 3). The excellent light transmittance may suggest that nanocellulose is easily dispersed in water.³¹ At higher drying temperatures (40 °C in this study), the nanofibrillated material did not redistribute homogeneously. This was due to the quicker film consolidation. In addition, high light transmittance is correlated with membrane transparency, which is related to their internal structure generated during the drying of the film.³² In addition, the membrane with PMVEMA-PEG only had light transmittance of 70% at 550 nm. The results indicate that the incorporation of 5 wt% TCS and TCL leads to a noticeable improvement for TCL in the optical transmittance

value of the PMVEMA-PEG-only membrane. In addition, the interference near the infrared region indicates high smoothness on the film surface and the uniformity of film thickness.³³

Contact angles

Short TOCN membranes (TCS) had a greater contact angle (67°) than the membranes constructed with long TOCNs/TCL (55°). In contrast, the PMVEMA-PEG-only membrane exhibits the maximum contact angle, notably measured as 69° (Fig. 4). In terms of fibril length, it appeared that shorter fibrils produced a greater contact angle than their longer counterparts. The length of nanocellulose significantly affected the surface structure. Compared to longer nanofibers, it was simpler to extract microparticles with a more compact, uniformly rough structure, and enhanced superhydrophobicity.³⁴ Low contact angle values indicate that water spreads and adheres to the surface, whereas high contact angle values indicate that the surface repels water.³⁵

Thermal stability

The thermal stability of TOCNs was affected by their length (Fig. 5 and Table 1). Long TOCNs in membrane matrices exhibited greater maximum degradation temperatures (T_{max}) and onset degradation temperatures (T_{on}) (Table 1). Because

decarboxylation occurs at lower temperatures,³⁶ the presence of sodium carboxylate groups in TOCNs influenced their thermal characteristics. At 100–130 °C, the weight loss was attributed to

dehydration, whereas at temperatures above 300 °C, it was attributed to polymer chain breakdown.³⁷

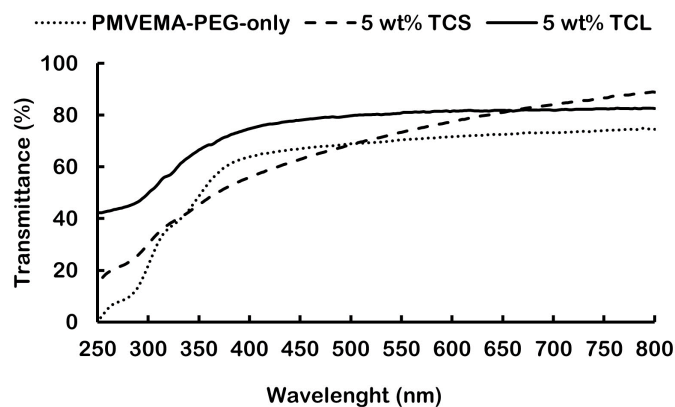


Figure 3: Transmittance of polymeric membranes composed of: PMVEMA-PEG-only (dotted line, data adopted from Hastuti *et al.*,²⁶ 5 wt% TCS (dashed line), and 5 wt% TCL (solid line)

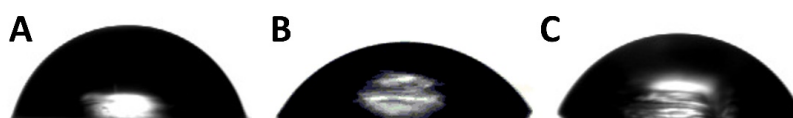


Figure 4: Contact angles of (A) PMVEMA-PEG-only, (B) membrane with 5 wt% TCL, and (C) membrane with 5 wt% TCS

The derivative weight curve (DTG) of PMVEMA-PEG-only and PMVEMA-PEG containing 5 wt% of both TCS and TCL showed three or four distinct peaks of T_{max} (Fig. 5). The first peak is associated with the dehydration of the diacids of PMVEMA. The second peak is associated with the combined decomposition of PMVEMA and PEG, and the third peak is attributed to the polymer chain degradation.³⁷ The length of TOCNs contributed to the thermal stability. The results showed that longer TOCNs in the PMVEMA-PEG matrix slightly increased thermal stability of the film by having higher maximum degradation temperatures (T_{max}). The onset temperatures (T_{on}) and maximum

degradation temperatures (T_{max}) are summarized in Table 1.

Mechanical properties and whiteness level

Figure 6 demonstrates that the membranes with longer TOCNs (TCL) exhibited greater tensile strength than the membranes with shorter TOCNs (TCS). During gelation, long TOCNs tend to entangle and increase the film's surface area. Due to the increased surface area, the distribution of force applied to the surface of the film was more dispersed than in the case of the surface of short fiber containing film. The tensile strength of longer fibers was higher (14 MPa) than that of shorter fibers (10 MPa).

Table 1
Thermal properties of membranes with short (TCS) and long (TCL) TOCNs

Sample	T_{max} (°C)	T_{on} (°C)
PMVEMA-PEG-only	151 ^a , 235 ^b , 408 ^c	107
5 wt% TCS	145 ^a , 222 ^b , 348 ^c , 404 ^d	134
5 wt% TCL	149 ^a , 229 ^b , 403 ^c	143

Note: ^afirst peak, ^bsecond peak, ^cthird peak, ^dfourth peak

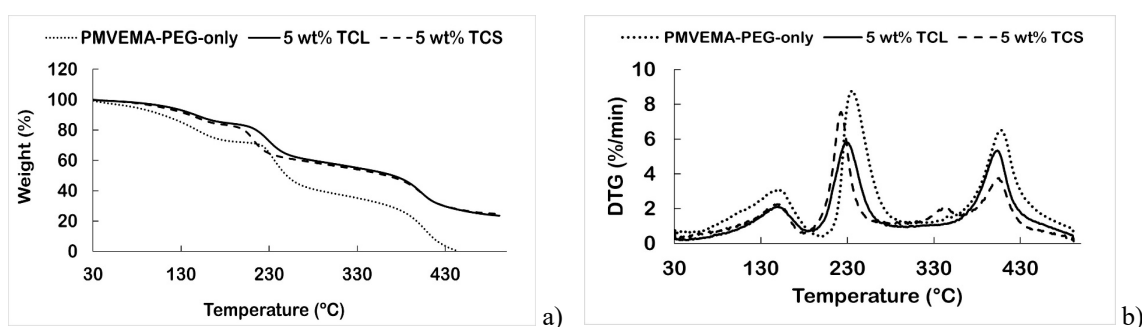


Figure 5: TGA (a) and DTG (b) curves of: PMVEMA-PEG-only, PMVEMA-PEG with 5 wt% TCL (solid line) and with 5 wt% TCS (dashed line)

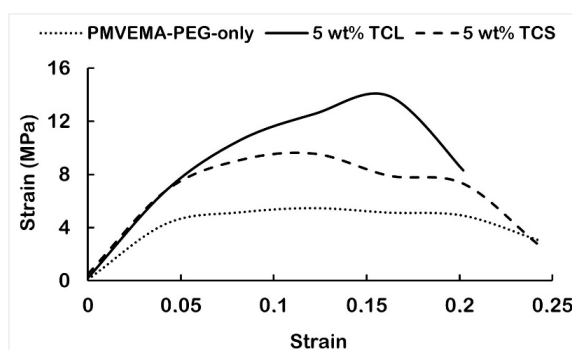


Figure 6: Tensile strength curves of membranes made of: PMVEMA-PEG-only (data adopted from Hastuti *et al.*²⁶), PMVEMA-PEG containing 5 wt% TCL (solid line) and PMVEMA-PEG containing 5 wt% TCS (dashed line)

This conclusion was consistent with previous findings published by Fukuzumi and colleagues.³⁸ This suggests that fiber length has an important role in influencing film properties, specifically tensile strength. In addition, the tensile strengths of the obtained films were higher compared to the previously reported study, which referred to PMVEMA-PEG foam and used high concentration of nanocellulose (>5%) as additive prepared by the directional freezing method.¹⁶ Cellulose nanofibers, specifically in the form of nanocellulose, exhibit superior performance as fillers in polymeric membranes compared to nanocellulose crystals, aligning with previous research findings.^{16,26} The presence of TOCNs,

which enhance polymeric membranes, aligns with our previous study findings. Adding TOCNs to alginate membranes doubled their tensile properties.³⁹

The process of color analysis involved the calculation of color differentiation. The total color differentiation (TCD), represented as ΔE , can be determined through the application of Equation 1. The term “color differentiation” in this study pertained to the color coordinate system known as CIE $L^*a^*b^*$, which was devised by the Commission Internationale de l’Eclairage (CIE). The outcomes of the TCD experiment are presented in Table 2.

Table 2
Whiteness level measurement

Sample	$(\Delta L^*)^2$	(Δa^*)	$(\Delta b^*)^2$	ΔE (to PMVEMA-PEG-only)
PMVEMA-PEG-only*	88.86	-0.55	18.61	n.d.
TCS5	92.34	-0.33	3.46	15.55
TCL5	91.07	0.51	2.56	16.24

*Data from a previous study (Hastuti *et al.*, 2020)²⁶; n.d. = not determined

The membrane with longer TOCNs (TCL) displayed a higher whiteness level (Δ^*L) than the membrane with shorter TOCNs (TCS). The levels of whiteness of the membranes incorporating TCL and TCS were 92.34 and 91.07, respectively (Table 2). According to Reddy and his co-authors, the total color differences increased linearly as the cellulose nanofiber concentration increased.⁴⁰

CONCLUSION

Five (5) wt% of TOCNs of varying lengths were added to the polymeric matrix, resulting in membranes with slightly varied characteristics. When longer TOCNs are utilized, somewhat higher transparency, thermal, and mechanical properties can be achieved. The amount of membrane roughness that can be estimated by the value of Ra demonstrated that the length of TOCNs did not significantly affect the level of membrane roughness.

ACKNOWLEDGEMENT: This research was supported by the Advanced Low Carbon Technology Research and Development Program from Japan Science and Technology Agency (T.K.). N.H. is grateful to Kementerian Pendidikan, Kebudayaan, Riset dan Pendidikan Tinggi, Republic of Indonesia, for partial financial support through an Unggulan Scholarship for 2016-2019.

REFERENCES

- H. Kargarzadeh, M. Mariano, J. Huang, N. Lin, I. Ahmad *et al.*, *Polymer*, **132**, 368 (2017), <https://doi.org/10.1016/j.polymer.2017.09.043>
- Z. Qazanfarzadeh and M. Kadivar, *Int. J. Biol. Macromol.*, **91**, 1134 (2016), <https://doi.org/10.1016/j.ijbiomac.2016.06.077>
- P. Hadi, M. Yang, H. Ma, X. Huang, H. Walker *et al.*, *J. Memb. Sci.*, **579**, 162 (2019), <https://doi.org/10.1016/j.memsci.2019.02.059>
- H. Fukuzumi, T. Saito, S. Iwamoto, Y. Kumamoto, T. Ohdaira *et al.*, *Biomacromolecules*, **12**, 11 (2011), <https://doi.org/10.1021/bm201079n>
- R. Endo, T. Saito and A. Isogai, *Polymer*, **54**, 2 (2013), <https://doi.org/10.1016/j.polymer.2012.12.035>
- Y. Habibi and A. Dufresne, *Biomacromolecules*, **9**, 7 (2008), <https://doi.org/10.1021/bm8001717>
- Y. Han, M. Yu and L. Wang, *Ind. Crop. Prod.*, **117**, 13 (2018), <https://doi.org/10.1016/j.foodhyd.2017.09.020>
- M. B. K. Niazi, Z. Jahan, S. S. Berg and Ø. W. Gregersen, *Carbohydr. Polym.*, **177**, 13 (2017), <https://doi.org/10.1016/j.carbpol.2017.08.125>
- J. D. Rusmirović, J. Z. Ivanović, V. B. Pavlović, V. M. Rakić, M. P. Rančić *et al.*, *Carbohydr. Polym.*, **164**,

- 64 (2017), <https://doi.org/10.1016/j.carbpol.2017.01.086>
- R. J. Moon, A. Martini, J. Nairn, J. Simonsen and J. Youngblood, *Chem. Soc. Rev.*, **40**, 7 (2011), <https://doi.org/10.1039/C0CS00108B>
- B. Deepa, E. Abraham, N. Cordeiro, M. Mozetic, A. P. Mathew *et al.*, *Cellulose*, **22**, 2 (2015), <https://doi.org/10.1007/s10570-015-0554-x>
- Q. Chen, Y. Liu and G. Chen, *Cellulose*, **26**, 4 (2019), <https://doi.org/10.1007/s10570-019-02254-x>
- D. Jun, Z. Guomin, P. Mingzhu, Z. Leilei, L. Dagang *et al.*, *Carbohydr. Polym.*, **168**, 255 (2017), <https://doi.org/10.1016/j.carbpol.2017.03.076>
- M. Sato, H. Ishii, Y. Sueda, K. Watanabe and D. Nagao, *Compos. Part C*, **5**, 100163 (2021), <https://doi.org/10.1016/j.jcomc.2021.100163>
- L. Goetz, A. Mathew, K. Oksman, P. Gatenholm and A. J. Ragauskas, *Carbohydr. Polym.*, **75**, 1 (2009), <https://doi.org/10.1016/j.carbpol.2008.06.017>
- L. Liang, C. Huang, N. Hao and A. J. Ragauskas, *Carbohydr. Polym.*, **213**, 346 (2019), <https://doi.org/10.1016/j.carbpol.2019.02.073>
- L. Goetz, M. Foston, A. P. Mathew, K. Oksman and A. J. Ragauskas, *Biomacromolecules*, **11**, 10 (2010), <https://doi.org/10.1021/bm1006695>
- A. Isogai, T. Saito and H. Fukuzumi, *Nanoscale*, **3**, 1 (2011), <https://doi.org/10.1039/C0NR00583E>
- T. Saito, M. Hirota, N. Tamura and A. Isogai, *J. Wood Sci.*, **56**, 3 (2010), <https://doi.org/10.1007/s10086-009-1092-7>
- A. Isogai and Y. Kato, *Cellulose*, **5**, 153 (1998), <https://doi.org/10.1023/A:1009208603673>
- T. Kitaoka, A. Isogai and F. Onabe, *Nord. Pulp Pap. Res. J.*, **14**, 4 (1999), <https://doi.org/10.3183/npprj-1999-14-04-p279-284>
- T. Saito, S. Kimura, Y. Nishiyama and A. Isogai, *Biomacromolecules*, **8**, 8 (2007), <https://doi.org/10.1021/bm0703970>
- T. R. Singh, P. McCarron, A. Woolfson and R. Donnelly, *J. Appl. Polym. Sci.*, **112**, 5 (2009), <https://doi.org/10.1002/app.29523>
- T. Zhang, J. Chen, Q. Zhang, J. Dou and N. Gu, *Colloid. Surfaces A Physicochem. Eng. Asp.*, **422**, 81 (2013), <https://doi.org/10.1016/j.colsurfa.2013.01.030>
- T. Saito and A. Isogai, *Biomacromolecules*, **5**, 5 (2004), <https://doi.org/10.1021/bm0497769>
- N. Hastuti, K. Kanomata and T. Kitaoka, *IOP Conf. Ser. Mater. Sci. Eng.*, **935**, 012051 (2020), <https://doi.org/10.1088/1757-899X/935/1/012051>
- B. K. Tiwari, K. Muthulumarappan, C. P. O'Donnell and P. J. Cullen, *J. Agric. Food Chem.*, **56**, 7 (2008), <https://doi.org/10.1021/jf073503y>
- S. Fujisawa, Y. Okita, H. Fukuzumi, T. Saito and A. Isogai, *Carbohydr. Polym.*, **84**, 1 (2011), <https://doi.org/10.1016/j.carbpol.2010.12.029>
- S. Rajesh, A. Jayalakshmi, S. Senthikumar, H. S. H. Sankar and D. R. Mohan, *Ind. Eng. Chem. Res.*, **50**, 24 (2011), <https://doi.org/10.1021/ie201181h>
- L. Kong, D. Zhang, Z. Shao, B. Han, Y. Lv *et al.*,

Desalination, **332**, 1 (2014),
<https://doi.org/10.1016/j.desal.2013.11.005>

³¹ K. Syverud, G. Chinga-Carrasco, J. Toledo and P. G. Toledo, *Carbohydr. Polym.*, **84**, 3 (2011),
<https://doi.org/10.1016/j.carbpol.2010.12.066>

³² R. Villalobos, J. Chanona, P. Hernández, G. Gutiérrez and A. Chiralt, *Food Hydrocoll.*, **19**, 1 (2005), <https://doi.org/10.1016/j.foodhyd.2004.04.014>

³³ M. Takahashi, K. Iyoda, T. Miyauchi, S. Ohkido, M. Tahashi *et al.*, *J. Appl. Phys.*, **106**, 044102 (2009),
<https://doi.org/10.1063/1.3204023>

³⁴ X. Zheng and S. Fu, *Colloid. Surfaces A Physicochem. Eng. Asp.*, **560**, (2019),
<https://doi.org/10.1016/j.colsurfa.2018.10.005>

³⁵ T. Huhtamäki, X. Tian, J. T. Korhonen and R. H. A. Ras, *Nat. Protoc.*, **13**, 1521 (2018),
<https://doi.org/10.1038/s41596-018-0003-z>

³⁶ H. Fukuzumi, T. Saito, Y. Okita and A. Isogai, *Polym. Degrad. Stab.*, **95**, 9 (2010),
<https://doi.org/10.1016/j.polymdegradstab.2010.06.015>

³⁷ S. S. Nair, J. Zhu, Y. Deng and A. J. Ragauskas, *ACS Sustain. Chem. Eng.*, **2**, 4 (2014),
<https://doi.org/10.1021/sc400445t>

³⁸ H. Fukuzumi, T. Saito and A. Isogai, *Carbohydr. Polym.*, **93**, 1 (2013),
<https://doi.org/10.1016/j.carbpol.2012.04.069>

³⁹ N. Hastuti, H. Setiawan, K. Kanomata and T. Kitaoka, *Cellulose Chem. Technol.*, **56**, 737 (2022),
<https://doi.org/10.35812/CelluloseChemTechnol.2022.56.65>

⁴⁰ J. P. Reddy and J. W. Rhim, *Carbohydr. Polym.*, **110**, 480 (2014),
<https://doi.org/10.1016/j.carbpol.2014.04.056>